Electronic Supplementary Material (ESI) for Physical Chemistry Chemical Physics.
This journal is © the Owner Societies 2021

Kinetics of the Gas Phase Reaction of the Criegee Intermediate CH_2OO with SO_2 as a Function of Temperature

Lavinia Onel,[1] Rachel Lade,[1] Jennifer Mortiboy,[1] Mark Blitz,[1,2] Paul Seakins,[1] Dwayne Heard,[1] and Daniel Stone[1*]

[1] School of Chemistry, University of Leeds, Leeds, LS2 9JT, UK

[2] National Centre for Atmospheric Science, University of Leeds, Leeds, LS2 9JT, UK

* Corresponding Author: d.stone@leeds.ac.uk, +44 113 343 6508

Supplementary Information

Determination of the reaction temperature

For the kinetic experiments at $T < 296$ K the reaction cell was immersed in a cooling bath of 30% ethane-1,2-diol in methanol with the assembly covered by 3 cm thick polystyrene. The temperature was controlled using a refrigerated immersion chiller (LabPlant Refrigerated Immersion Probe, RP-100CD) with the probe immersed in the cooling mixture. The cooling bath was mixed using magnetic stirring at both ends of the bath to achieve a constant temperature, within 98%, along the length of the bath. The temperature in the reaction cell was determined through measurements of the absorption spectra for NO_2 + N_2O_4 mixtures recorded in the range 250–665 nm using the single pass optical arrangement after the kinetic experiments at each temperature between 223 K and 281 K. This method offers the potential to determine the mean temperature along the length of the reaction cell under identical flow conditions to those used in kinetics experiments, and can be used at sub-ambient temperatures where there is significant concentration of N_2O_4.

Reference spectra for NO_2[1] and N_2O_4[1] were fit to the observed absorbance spectra using equation ES1 to obtain the concentrations of NO_2 and N_2O_4.

$$A(\text{tot})_\lambda = \ln\left(\frac{I_{\lambda,0}}{I_\lambda}\right) = \sigma_{NO2,\lambda}\,[NO_2]\,l + \sigma_{N2O4,\lambda}\,[N_2O_4]\,l \qquad \text{(ES1)}$$

where $A(\text{tot})_\lambda$ is the total measured absorbance at wavelength λ, $I_{\lambda,0}$ is the background intensity at wavelength λ, measured in the absence of NO_2 and N_2O_4, I_λ is the intensity in the presence of NO_2 + N_2O_4 at wavelength λ, $\sigma_{NO2,\lambda}$ and $\sigma_{N2O4,\lambda}$ are the cross-sections of NO_2 and N_2O_4, respectively at wavelength λ, and l is the absorption pathlength given by the cell length of 100 cm. Concentrations were determined to be in the ranges: $[NO_2] = (0.5 – 5.0) \times 10^{16}$ molecule cm^{-3} and $[N_2O_4] = (0.1 – 5.8) \times 10^{15}$ molecule cm^{-3}. Figure S1 shows a typical fit to the observed absorbance.

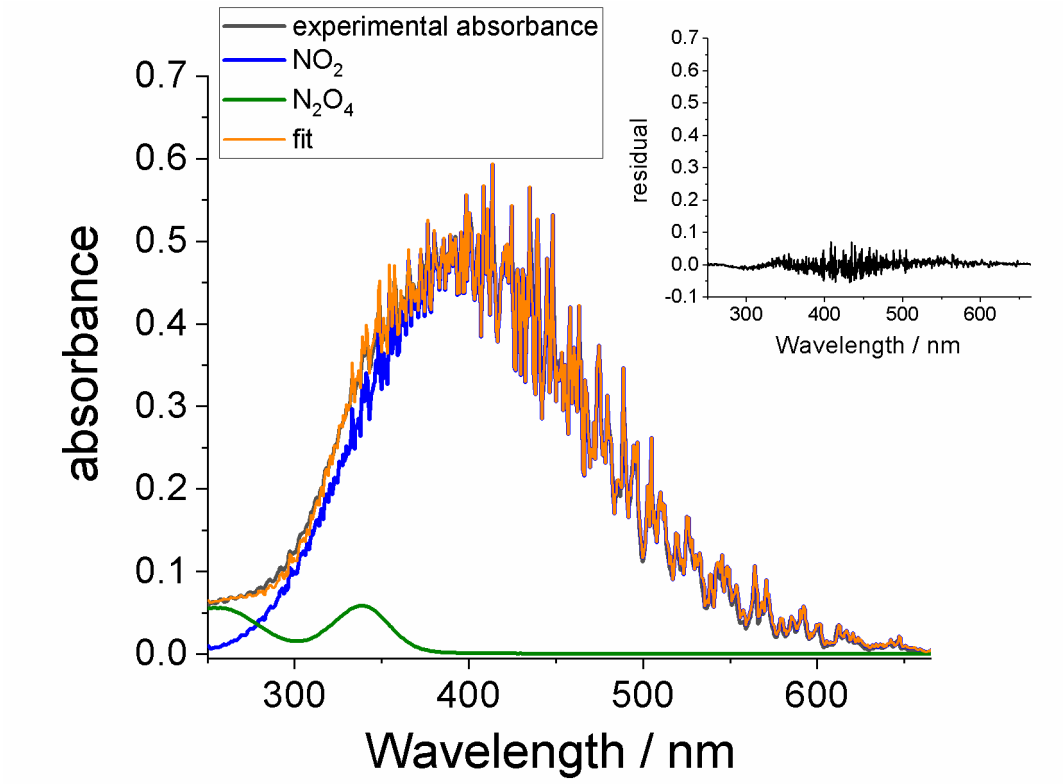

Figure S1. Measured absorbance (black), total fit (orange), and individual contributions from NO_2 (blue) and N_2O_4 (green) determined fitting reference absorption cross-sections to the observed absorbance using equation ES1. The determined concentrations are: $[NO_2] = 7.7 \times 10^{15}$ molecule cm^{-3} and $[N_2O_4] = 8.6 \times 10^{14}$ molecule cm^{-3}. Equations ES2 and ES3 give $T = 253$ K.

The equilibrium constant, K_c, for the dimerisation reaction $2NO_2 \rightleftarrows N_2O_4$ was determined using equation ES2.

$$K_c = \frac{[N_2O_4]}{[NO_2]^2} \qquad \text{(ES2)}$$

The temperature was then derived from knowledge of the temperature dependence of K_c described by equation ES3.[2]

$$K_c \,/\, \text{cm}^3 \text{ molecule}^{-1} = 5.9\times10^{-29} \text{cm}^3 \text{ molecule}^{-1} \exp\left(\frac{6643 \text{ K}}{T \,/\, \text{K}}\right) \qquad \text{(ES3)}$$

Equation ES3 shows that decreasing the temperature K_c increases owing to the shift of the dimerisation equilibrium to N_2O_4 formation: $K_c(296 \text{ K}) = 3.6 \times 10^{-19}$ cm^3 molecule^{-1} and $K_c(223 \text{ K}) = 5.1 \times 10^{-16}$ cm^3 molecule^{-1}.

For experiments at $T \geq 295$ K, a jacketed reaction cell was used in which the temperature was controlled by circulating thermofluid (HUBE6479 DW-therm oil) from a thermoregulator (Huber Unistat 360). For these experiments the temperature in the cell was calibrated for a given pressure, flow rate of N_2, and temperature setting in separate experiments to those used to determine kinetics. The calibration was performed using a K-type thermocouple placed in the centre of the radius of the reaction cell at 5 cm intervals along the length of the cell. For given conditions, the measured temperature reached a constant value within 5-10 cm of the entry point of the gas to the cell and the average temperature along the length of the cell determined by integration of the measured temperature profile.

Typical uncertainties in the temperatures for experiments below room temperature (obtained from the NO_2/N_2O_4 measurements) were on the order of 5 K at the lowest temperature of 223 K, where the uncertainty is greatest. At the lowest temperature, the difference between the temperature within the reaction and the bath temperature was 12 K. Typical uncertainties in the temperatures for experiments above room temperature (obtained from the thermocouple measurements) were on the order of 6 K at the highest temperature of 344 K, again where the uncertainty is greatest. At the highest temperature, the difference between the temperature within the reaction and the temperature measured inside the Huber unit was 9 K.

Determination of the effective absorption pathlength in kinetic measurements

The probe light was aligned in a 7 pass arrangement along the length of the reaction cell using 8 Al-enhanced mirrors (Knight Optical, UK), each of 12 mm diameter. The mirror arrangement was set up to optimise the overlap of the probe beam with the photolysis laser beam and has been described in previous work.[3-5] The total effective pathlength was determined using the depletion of $[CH_2I_2]$ by photolysis at 248 nm (RS1), $\Delta[CH_2I_2]$, determined from the measured concentration of CH_2I_2 prior to photolysis and the laser fluence in the cell, and $\Delta[CH_2I_2] \times l$ derived from analysis of the absorption spectra obtained following photolysis.

$$CH_2I_2 + h\nu \rightarrow CH_2I + I \qquad \text{(RS1)}$$

The the depletion of $[CH_2I_2]$ was given by equation ES4.

$$\Delta[CH_2I_2] = f_{248\ nm}\ \sigma_{CH2I2,\ 248\ nm}\ [CH_2I_2]_0 \qquad \text{(ES4)}$$

where $f_{248\ nm}$ is the laser fluence in the cell (Table S1), $\sigma_{CH2I2,\ 248\ nm} = 1.6 \times 10^{-18}$ cm^2 molecule^{-1} is the cross-section of CH_2I_2 at 248 nm,[2] and $[CH_2I_2]_0$ is the pre-photolysis concentration of CH_2I_2 which was measured in separate absorption measurements before and after each experiment to determine k_3.

The fit of the equation E1 in the main text to the absorption spectra gave $\Delta[CH_2I_2] \times l$, which was then divided by $\Delta[CH_2I_2]$ obtained by equation ES4 to determine $l = (471 \pm 50)$ cm (where the error is at the 2σ level). Table S1 shows the individual values obtained for l from 11 measurements. A typical $\Delta[CH_2I_2] \times l$ vs. time profile obtained from E1 (main text) is shown in Figure S2.

$f_{248\ nm}$ / photon cm^{-2}	$[CH_2I_2]_0$ / 10^{13} molecule cm^{-3}	$\Delta[CH_2I_2]$ / 10^{12} molecule cm^{-3}	$\Delta[CH_2I_2] \times l$ / 10^{14} molecule cm^{-2}	l /cm
3.9	1.9	1.2	5.0	431
3.9	1.8	1.1	4.9	446
3.9	1.2	0.8	3.6	470
3.9	1.1	0.6	3.4	524
3.9	2.7	1.6	7.7	477
4.3	5.0	3.4	16	470
4.3	4.8	3.2	16	485
4.3	4.8	3.2	15	458
4.3	4.8	3.2	15	458
4.3	4.8	3.2	15	466
2.3	4.3	1.6	7.7	494

Table S1. Effective absorption pathlength, l determinations using $\Delta[CH_2I_2]$ given by equation ES4 and $\Delta[CH_2I_2] \times l$ obtained by the fit of equation E1 (main text) to the UV absorption spectra recording during the kinetic experiments.

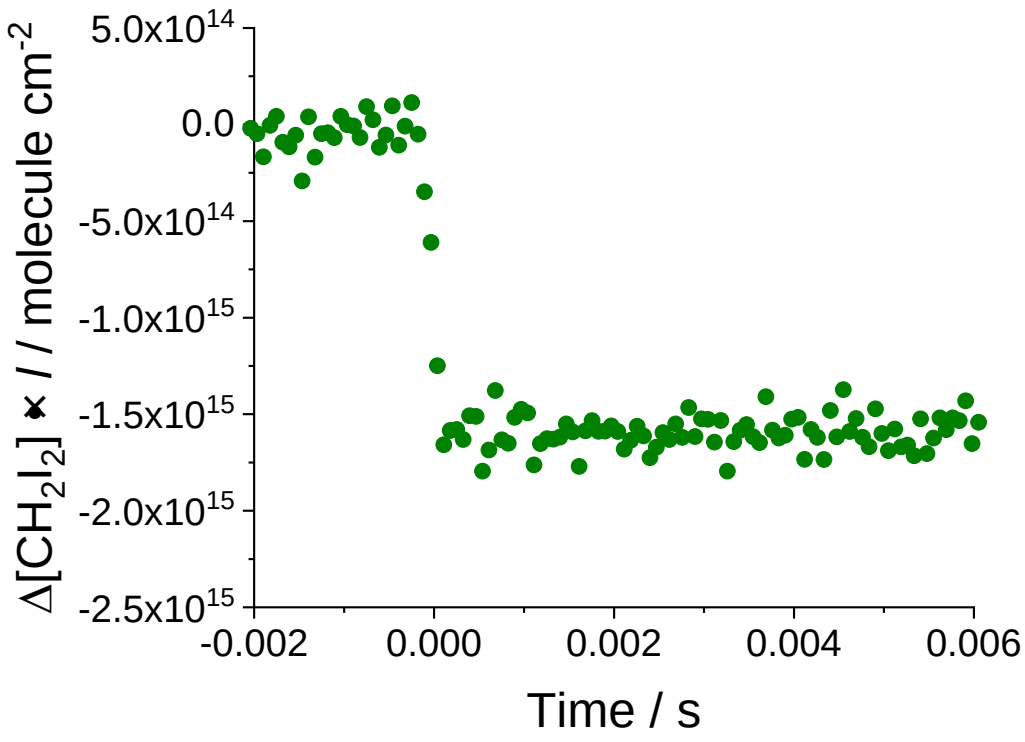

Figure S2. Time profile of the product between the depleted CH_2I_2 concentration by photolysis and the pathlength in the UV absorption experiments, $\Delta[CH_2I_2] \times l$ for $[CH_2I_2]_0 = 4.8 \times 10^{13}$ molecule cm^{-3} and in the absence of SO_2 at 295 K and 85 Torr mixture of O_2:N_2 = 1:3. The points at times $t < 0$ are pre-photolysis data.

Experimental conditions

Experiments were performed for the range of conditions shown in Table S2.

T / K	$[CH_2I_2]_0$ / 10^{13} molecule cm^{-3}	$[SO_2]_0$ / 10^{13} molecule cm^{-3}	$[CH_2OO]_0$ / 10^{12} molecule cm^{-3}
223	3.4	0.5 – 2.4	2.0
259	6.0	1.9 – 5.0	2.6
266	2.6	1.2 – 5.5	1.0
270	5.0	0.6 – 4.5	1.5
275	2.3	0.8 – 4.5	0.7
281	2.3	1.2 – 5.2	0.9
296	1.2	0.7 – 4.2	0.4
316	4.2	0.5 – 3.1	1.6
324	5.4	0.8 – 3.6	1.5
331	7.4	1.0 – 5.1	1.1
340	4.6	0.9 – 3.0	1.6
344	4.5	0.6 – 3.2	1.4

Table S2. Experimental conditions used in the kinetic experiments. For all experiments p = 85 Torr.

Bimolecular plots

Figure S3 shows the bimolecular plots, k_{obs} vs. [SO_2], for each temperature investigated in this work. The pressure was 85 Torr at all temperatures.

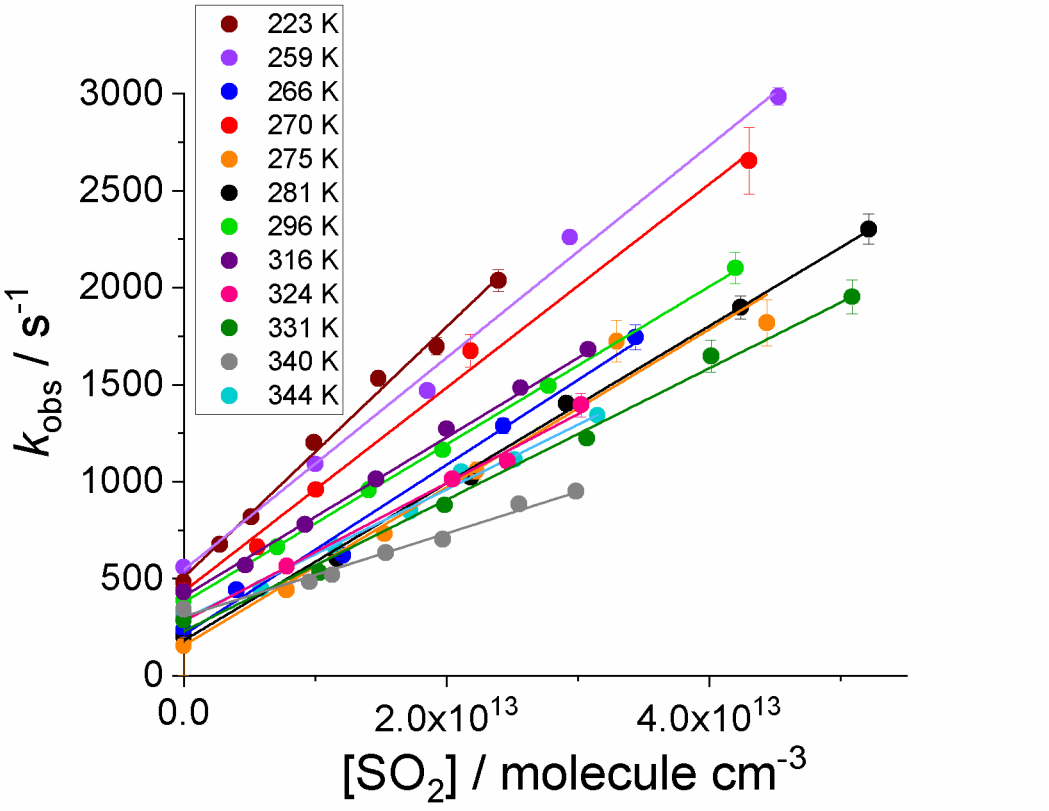

Figure S3. k_{obs} vs. [SO_2] plots at 85 Torr and all employed temperatures in the range 223 – 344 K. The linear fits to data result in the second order rate coefficients k_3 for each temperature: (6.4 ± 0.3) × 10^{-11} cm^3 $molecule^{-1}$ s^{-1} (223 K, dark brown), (5.5 ± 0.3) × 10^{-11} cm^3 $molecule^{-1}$ s^{-1} (259 K, light violet), (4.4 ± 0.3) × 10^{-11} cm^3 $molecule^{-1}$ s^{-1} (266 K, blue), (5.3 ± 0.3) × 10^{-11} cm^3 $molecule^{-1}$ s^{-1} (270 K, red), (4.1 ± 0.5) × 10^{-11} cm^3 $molecule^{-1}$ s^{-1} (275 K, orange), (4.1 ± 0.1) × 10^{-11} cm^3 $molecule^{-1}$ s^{-1} (281 K, black), (4.0 ± 0.1) × 10^{-11} cm^3 $molecule^{-1}$ s^{-1} (296 K, light green), (4.2 ± 0.1) × 10^{-11} cm^3 $molecule^{-1}$ s^{-1} (316 K, dark violet), (3.6 ± 0.2) × 10^{-11} cm^3 $molecule^{-1}$ s^{-1} (324 K, pink), (3.4 ± 0.1) × 10^{-11} cm^3 $molecule^{-1}$ s^{-1} (331 K, olive), (2.2 ± 0.1) × 10^{-11} cm^3 $molecule^{-1}$ s^{-1} (340 K, grey), and (3.3 ± 0.1) × 10^{-11} cm^3 $molecule^{-1}$ s^{-1} (344 K, light blue). For each temperature [CH_2I_2] was constant (Table S2).

Concentration-time profiles for IO

Figure S4 shows typical concentration-time profiles obtained for CH_2OO and IO from fits to the total observed absorbance following photolysis of $CH_2I_2/O_2/N_2/SO_2$ mixtures. IO radicals are formed in the system as a result of secondary chemistry,[4,5] but do not influence the results reported here for $CH_2OO + SO_2$.

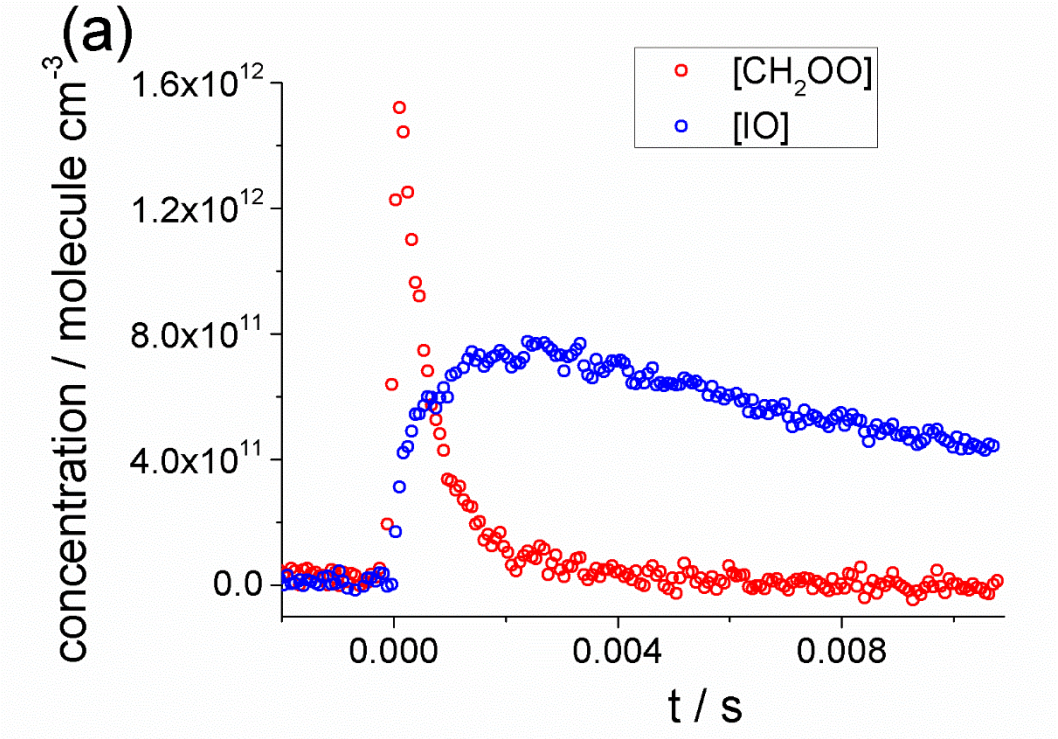

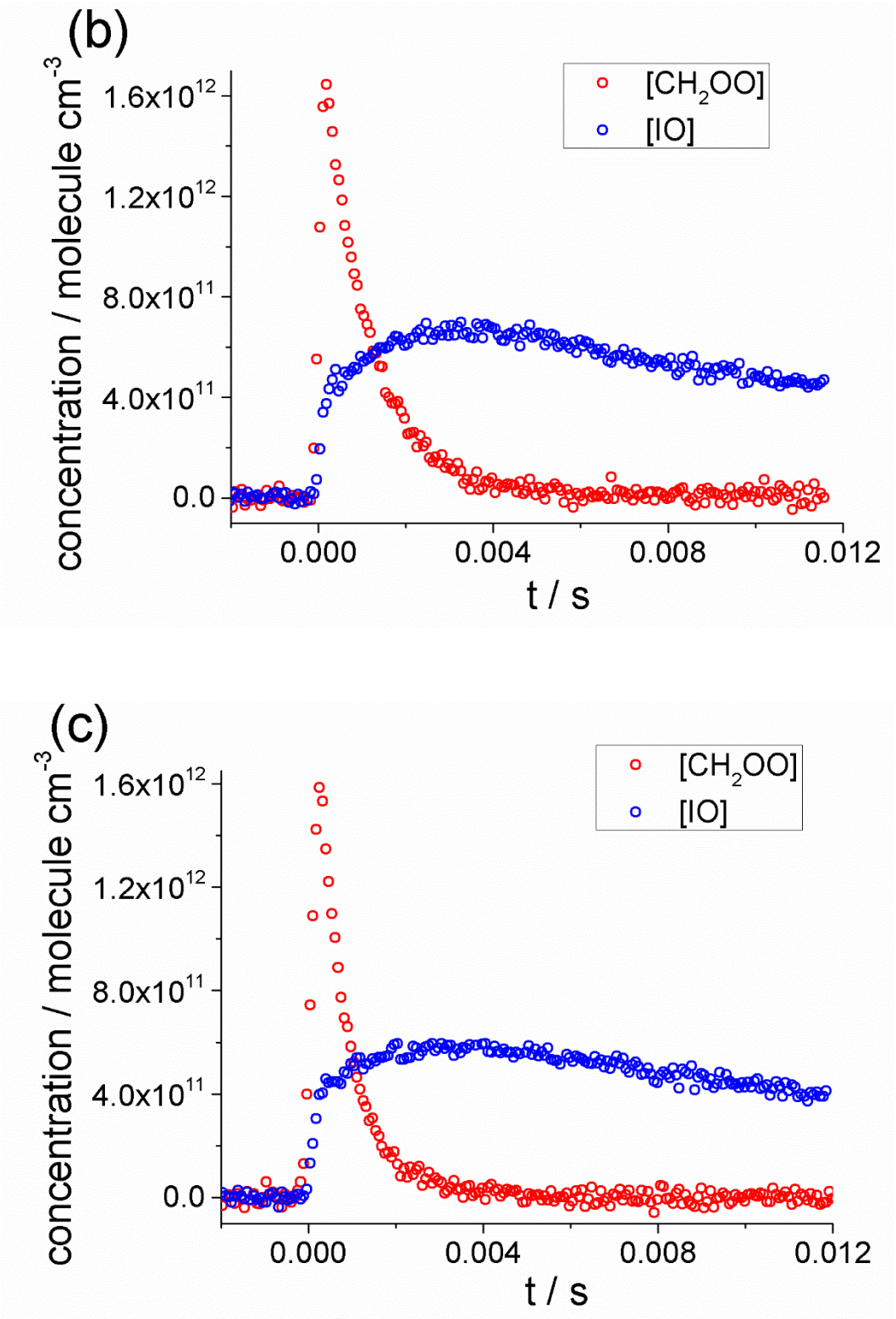

Figure S4. Typical concentration-time profiles for CH_2OO (red) and IO (blue) obtained from fits to the total absorbance following photolysis of $CH_2I_2/O_2/N_2/SO_2$ mixtures at 85 Torr and (a) 223 K, (b) 296 K and (c) 316 K.

References

1. Vandaele, A. C.; Hermans, C.; Simon, P. C.; Carleer, M.; Colin, R.; Fally, S.; Merienne, M. F.; Jenouvrier, A.; Coquart, B., Measurements of the NO_2 absorption cross-section from 42 000 cm(-1) to 10 000 cm(-1) (238-1000 nm) at 220 K and 294 K. *Journal of Quantitative Spectroscopy & Radiative Transfer* **1998,** *59* (3-5), 171-184.
2. Burkholder, J. B., Sander, S. P., Abbatt, J. P. D., Barker, J. R., Huie, R. E., Kolb, C. E., Kurylo, M. J., Orkin, V. L., Wilmouth, D. M., Wine, P. H., Chemical kinetics and photochemical data for use in atmospheric studies - Evaluation No. 18. JPL Publication 15-10: available at: http://jpldataeval.jpl.nasa.gov/, last access: 15 July 2020, 2015.
3. Lewis, T.; Heard, D. E.; Blitz, M. A., A novel multiplex absorption spectrometer for time-resolved studies. *Review of Scientific Instruments* **2018,** *89* (2).
4. Mir, Z. S.; Lewis, T. R.; Onel, L.; Blitz, M. A.; Seakins, P. W.; Stone, D., CH_2OO Criegee intermediate UV absorption cross-sections and kinetics of CH_2OO + CH_2OO and CH_2OO + I as a function of pressure. *Physical Chemistry Chemical Physics* **2020,** *22* (17), 9448-9459.
5. Onel, L.; Blitz, M.; Seakins, P.; Heard, D.; Stone, D., Kinetics of the Gas Phase Reactions of the Criegee Intermediate CH_2OO with O_3 and IO. *J. Phys. Chem. A* **2020,** *124* (31), 6287-6293.